

A Weakly Antiferromagnetically Coupled Biradical Combining Verdazyl with Nitronyl Nitroxide Units

Pavel V. Petunin,^[a, b] Tatyana V. Rybalova,^[c, d] Marina E. Trusova,^[a] Mikhail N. Uvarov,^[d, e] Maxim S. Kazantsev,^[c] Evgeny A. Mostovich,^[d] Lars Postulka,^[f] Paul Eibisch,^[f] Bernd Wolf,^[f] Michael Lang,^[f] Pavel S. Postnikov,^{*[a]} and Martin Baumgarten^{*[g]}

An antiferromagnetically (AFM) coupled biradical based on oxoverdazyl and nitronyl nitroxide was synthesized in 46% yield using Sonogashira coupling. The obtained heterobiradical evidenced distinct properties of both radical entities in solution. Depending on the solvent, the prepared biradical crystallized in two different forms. SQUID magnetization measurements on Form II showed coupling constants $J_{\text{intra}}/k_B = -2.1$ K and $zJ_{\text{inter}}/k_B = -11.5$ K. Consequently, total intermolecular exchange interactions are five times larger than the intramolecular ones. Further, DFT calculations explained this phenomenon and indicated the advantage of Form I for further in-depth investigations.

Weakly antiferromagnetically coupled (AFM) crystalline spin- $1/2$ dimers can serve to investigate critical phenomena such as the formation of triplon excitations and their interactions in a magnetic field strong enough to close the singlet-triplet gap of the biradicals. Depending on the interdimer exchange interaction (J_{inter}) relative to the intradimer exchange interaction (J_{intra}) different dimensionalities of spin systems in a crystalline solid can be observed, such as one-dimensional (1D) spin-ladder systems showing Luttinger-liquid behavior,^[1] two-dimensional (2D) Berezinskii-Kosterlitz-Thouless networks,^[2] or three-dimensional (3D) Bose-Einstein condensation (BEC) of triplon excitations.^[3] Therefore a control of J_{intra} as well as J_{inter} is essential and we have shown earlier that this is possible in organic biradicals, where the intramolecular interactions can be fine-tuned through the applied spacer between the radical units.^[4] Besides changing the bridge between the two radical units, two different stable radicals can also be applied for varying the exchange interaction with a given spacer as exhibited for a tetramethoxypyrene with mixed nitronyl nitroxide and iminonitroxide.^[5] Earlier, we tested two nitronyl nitroxides (NN) depicted as **A**^[6,7] in Figure 1 and two iminonitroxides (IN) shown as **B**^[8] with a tolane bridge (1,2-bis(phenyl) acetylene) for achieving 2D and 3D ordering of triplon excitations of these spin dimers in the crystal lattice. Therefore in the present work, we consider a combination of nitro-

- [a] Dr. P. V. Petunin, Dr. M. E. Trusova, Dr. P. S. Postnikov
Research School of Chemistry & Applied Biomedical Sciences
National Research Tomsk Polytechnic University
30 Lenin ave.
Tomsk 634050 (Russia)
E-mail: postnikov@tpu.ru
- [b] Dr. P. V. Petunin
Department of Chemistry
Siberian State Medical University
2 Moskovskiy trakt
Tomsk 634050 (Russia)
- [c] T. V. Rybalova, Dr. M. S. Kazantsev
N.N. Vorozhtzov Novosibirsk Institute of Organic Chemistry of Siberian Branch of Russian Academy of Sciences
9 Lavrent'ev ave.
Novosibirsk 630090 (Russia)
- [d] T. V. Rybalova, Dr. M. N. Uvarov, Dr. E. A. Mostovich
Novosibirsk State University
2, Pirogova str.
Novosibirsk 630090 (Russia)
- [e] Dr. M. N. Uvarov
V. V. Voevodsky Institute of Chemical Kinetics and Combustion, Siberian Branch, Russian Academy of Sciences
3, Institutskaya str.
Novosibirsk 630090 (Russia)
- [f] Dr. L. Postulka, P. Eibisch, Dr. B. Wolf, Prof. Dr. M. Lang
Physikalisches Institut
Goethe Universität Frankfurt
1, Max von Laue Str.
60438 Frankfurt am Main (Germany)
- [g] Prof. Dr. M. Baumgarten
Max Planck Institute for Polymer Research
10, Ackermannweg, 55128 Mainz (Germany)
E-mail: baumgart@mpip-mainz.mpg.de

© 2019 The Authors. Published by Wiley-VCH Verlag GmbH & Co. KGaA. This is an open access article under the terms of the Creative Commons Attribution License, which permits use, distribution and reproduction in any medium, provided the original work is properly cited.

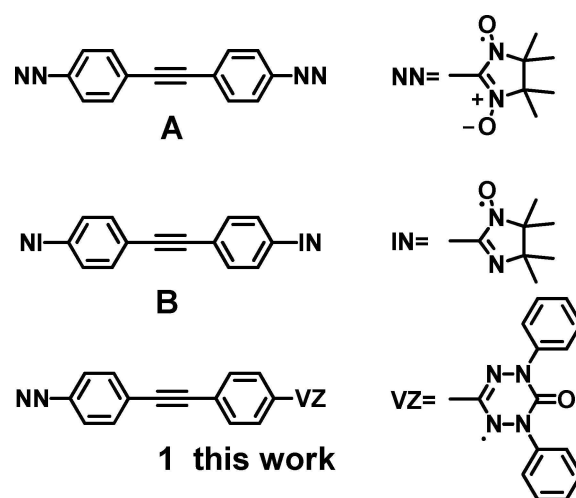
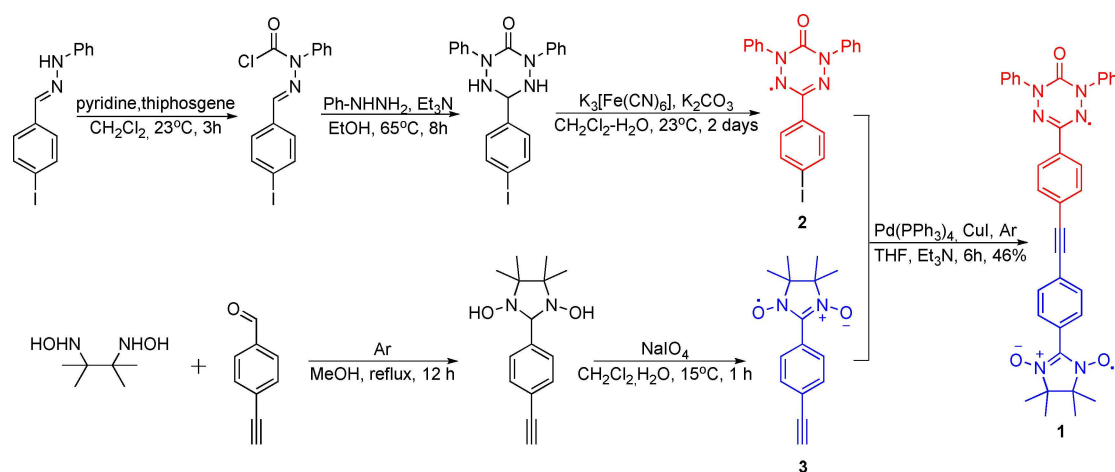


Figure 1. Homobiradicals **A** and **B** and the newly designed heterobiradical **1** with tolane bridge.



Scheme 1. Synthetic pathway for the preparation of hetero-biradical 1.

nylnitroxide (NN) and oxoverdazyl radicals (VZ), which is derived from the described homobiradicals A and B (Figure 1). While it is difficult to achieve such a hetero-biradical upon two different kinds of condensation of dialdehyde precursors, Sonogashira coupling between the two different radical fragments is considered as a prospective pathway.

The hetero-biradical 1 was prepared by using a convergent approach that included the reaction between ethynyl- and iodo-substituted radicals (Scheme 1). Both building blocks were synthesized *via* well-established procedures: verdazyl 2 was prepared from 4-iodobenzaldehyde *via* published method^[9] and the NNR 3 was synthesized according to Klyatskaya et al.^[10]

The most intriguing issue in the synthesis of the desired biradical was the reaction between the two building blocks. We previously reported the evaluation of Pd-catalysed coupling reactions, where the iodine-substituted 6-oxoverdazyl 2 exhibited higher activity in Sonogashira reaction than appropriate Kuhn-verdazyls.^[9,11] Therefore we chose this substrate as an iodine-containing moiety for further coupling. The Sonogashira cross-coupling reaction between radicals 2 and 3 was realized according to previously published conditions.^[11] The reaction proceeded with the formation of a target product in the mixture of NNR by-products and due to this reason, good yield of the desired biradical 1 was achieved only in case of addition of 1.5 eq. of NNR 3. Finally, hetero-bi-radical 1 was isolated by column chromatography. Detailed information about the synthesis of the starting materials and the heterobiradical 1 is presented in Section S1 of the Supporting Information.

The electronic properties of the prepared radical 1 were evaluated using UV-Vis spectroscopy and cyclic voltammetry (CV) measurements. The electronic spectrum shows absorption bands with maxima around 555, 590 nm and 380, 650 nm, which are in accordance with the absorbance of verdazyl and NNR moieties, respectively (Section S2 in the Supporting Information). The 500–750 nm region in the UV-Vis spectrum of 1 demonstrated weak $n-\pi^*$ band ($\epsilon \approx 450 \text{ cm}^{-1} \text{ M}^{-1}$) of the NN radical (Section S2). The heterobiradical 1 was also studied by CV measurements (Section S3). We observed two reversible

reduction waves and one intensive reversible oxidation wave with a broad shoulder. The appearance of a broad peak is due to close energies of the SOMO in verdazyl and the NN moieties. The resulting differences between E_{ox}^1 and E_{ox}^2 potentials are less than 0.1 V. As a result, two redox processes overlapped around 0.45 V. At the same time the reduction processes for verdazyl and NN were well-resolved and had a good agreement with reduction potentials of 2 and 3 as starting materials ($E_{\text{red}}^1(\text{NN}) = -1.38 \text{ V}$ and $E_{\text{red}}^2(\text{VZ}) = -1.01 \text{ V}$, Section S3).

The EPR spectrum of 1 in toluene solution exhibited the complex pattern (SI Section S4), which is typical for hetero-radical systems.^[12–14] Heterobiradical demonstrated a g -value of 2.0050 – an average between $g = 2.0038$ of VZ and $g = 2.0067$ of NN radicals.

The crystallisation of biradical 1 was successful under different conditions enabling the isolation of two different crystal solvates (Figure 2, SI Section 5). The first one (Form I) was obtained by slow evaporation at room temperature from 1:1 v/v DCM : hexane mixture (Figure 2 top). The second (Form II, Figure 2 bottom) was formed via slow diffusion of hexane into chloroform – toluene mixture (20:1, v:v).

The main difference between the crystal structures is governed by the different interplanar angles between the phenylene moieties in the toluene linker and the resulting angles between the two radical planes (see SI Section 5). Form I is closer to a planar structure (21° between planes of VZ and NN) as compared to Form II (78° between planes of VZ and NN). The structural parameters (bond length and angles) in radical moieties were similar with typical values in verdazyl and nitronyl-nitroxide monoradicals. Thus, crystallisation from different solvents could be applied to fine-tune the intramolecular interactions within the biradical 1 skeleton. This effect potentially could be used for controlling magnetic properties of the studied materials.

The magnetic properties of Form II single crystals were measured with a SQUID magnetometer within a temperature range of $2 \text{ K} \leq T \leq 270 \text{ K}$ at a field of $B = 1 \text{ T}$ (Figure 3). The $\chi_{\text{mol}} T$ vs. T plot is shown in the inset, indicating an overall

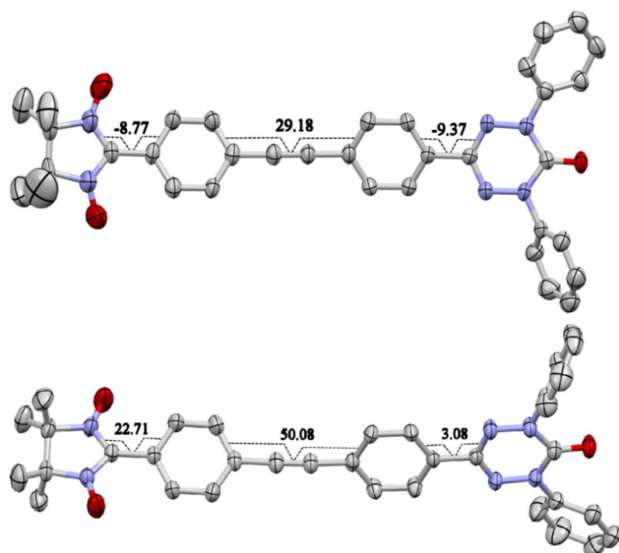


Figure 2. X-Ray structure of **1** (Form I – top, Form II – bottom) and the values of the dihedral angles between the planes of phenyl, VZ and NN moieties. Thermal ellipsoids are drawn at 50% probability.

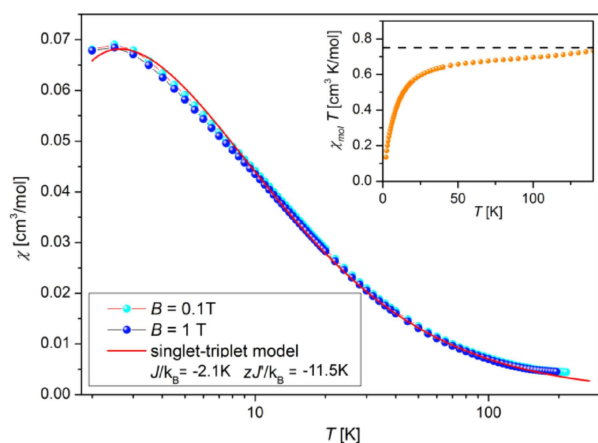


Figure 3. Molar susceptibility vs. Temperature in the range 2–220 K and field strengths of 0.1 T (light blue full circles) and 1 T (dark blue circles) together with a fit according to the model discussed in text. The inset shows a $\chi_{mol} T$ vs. T plot (full orange circles) with a high temperature value of $0.75 \text{ cm}^3 \text{ K/mol}$ (black dotted line).

antiferromagnetic exchange, while the main plot χ_{mol} vs. T clearly shows a maximum at 2.5 K.

To analyse the SQUID data a coupled model dimer was used. Combined with a singlet-triplet model the experimental data can be reproduced by taking an inter-dimer coupling into account within a mean-field approximation. As shown in Figure S11 of the SI a very weak intradimer coupling of $J_{intra}/k_B = -2.1 \text{ K}$ can be extracted from the field dependence at different temperatures. At the same time, the data fits to a total susceptibility curve yield $zJ_{inter}/k_B = -11.5 \text{ K}$ with z as the number of nearest neighbours. Thus, the total intermolecular interaction is five times larger than the intramolecular exchange, which is not well-suited to reach higher dimensionalities of the spin ordered triplons in a magnetic field.

Recently DFT methods were successfully applied to calculate spin-spin interactions and explain experimental data.^[8,14,15]

We performed DFT calculations to estimate the spin-density distribution and the strength of intra- and intermolecular exchange interactions in this biradical. The geometries of the X-ray structures were used for model calculations. The Heisenberg-Dirac-Van Vleck (HDVV) Hamiltonian as proposed by Noodleman was applied.^[17,18] The broken-symmetry (BS) approach from Yamaguchi^[19,20] was then used for elucidation of the exchange interaction J , which becomes, $J/k_B = (E(\text{BS}) - E(\text{T})) / (S^2(\text{T}) - S^2(\text{BS}))$, $E(\text{BS})$ and $E(\text{T})$ being the energy of the broken symmetry and the triplet energy, respectively. S^2 are the eigenvalues of the spin operator. With $S^2(\text{BS})$ close to 1 and $S^2(\text{T})$ close to 2, the direct exchange becomes $J/k_B = E(\text{BS}) - E(\text{T})$.

Furthermore, the singlet and triplet energy level calculations were carried out using the UBLYP hybrid functional with 6–31G (d) basis set to avoid Hartree-Fock contamination, which usually leads to larger spin alternations. The intramolecular exchange interactions (J/k_B) differed strongly between the two crystal solvates. The values of exchange coupling corresponding to Form I and Form II were $J_{intra}/k_B = -2.94 \text{ cm}^{-1} = -4.23 \text{ K}$ and $J_{intra}/k_B = -1.54 \text{ cm}^{-1} = -2.2 \text{ K}$, respectively (Figure S10). The decrease of J_{intra} compared to J_{intra} is easily assigned to the large interplanar angle between the radical units (78°) in Form II (Figure 2) reducing the spin-spin interaction. For calculation of the interdimer interaction, the X-ray dimer structure geometries of both forms were selected, and the one with more distant radical site on each biradical was deleted (see SI Section S6). For Form I, two closely overlapping VZ radicals were found within a short distance providing $J_{inter}/k_B = -2.13 \text{ cm}^{-1} = -3.06 \text{ K}$, which should enable a decent increase of the dimensionality of the triplon excitations in the crystal lattice. For Form II, two NN radical fragments are closely packed, with a relatively short NO-ON separation of 4.38 \AA dominating this exchange interaction and leading to a larger $J_{inter}/k_B = -4.39 \text{ cm}^{-1} = -6.3 \text{ K}$.

From the calculations, it thus appears that Form I would be much more promising than Form II, and larger crystalline amounts of Form I would be needed.

In conclusion, we have developed an approach for preparing AFM coupled heterobiradical based on oxoverdazyl and nitronylnitroxide *via* Sonogashira coupling. This pathway shows high potential for further design of tolane-bridged hetero-spin systems. Both radical moieties have distinctly different optical and redox properties, and verdazyls are slightly less spin delocalised to the bridging unit than nitronylnitroxides, thus reducing the exchange interaction. The obtained biradical crystallizes into two solvates that have principally different magnetic properties: Form II leads to larger intermolecular than intramolecular exchange interactions, which is reversed in Form I. Consequently, synthesized heterobiradical in Form I is a prospective material for further investigations of interacting triplons in a magnetic field.

Acknowledgements

This work was supported by the Russian Ministry of Education and Science (Scientific Program no. 4.5924.2017) and the DFG-TR49 project. P.V.P. and P.S.P. would like to acknowledge the Multi-Access Chemical Research Center SB RAS for spectral and analytical measurements. Open access funding enabled and organized by Projekt DEAL.

Conflict of Interest

The authors declare no conflict of interest.

Keywords: antiferromagnetism · multispin systems · magnetic properties · radicals · Sonogashira coupling

- [1] C. Rüegg, K. Kiefer, B. Thielemann, D. F. McMorro, V. Zapf, B. Normand, M. B. Zvonarev, P. Bouillot, C. Kollath, T. Giamarchi, S. Capponi, D. Poilblanc, D. Biner, K. W. Krämer, *Phys. Rev. Lett.* **2008**, *101*, 247202.
- [2] U. Tutsch, B. Wolf, S. Wessel, L. Postulka, Y. Tsui, H. O. Jeschke, I. Opahle, T. Saha-Dasgupta, R. Valentí, A. Brühl, K. Remović-Langer, T. Kretz, H.-W. Lerner, M. Wagner, M. Lang, *Nat. Commun.* **2014**, *5*, 5169.
- [3] T. Giamarchi, C. Rüegg, O. Tchernyshyov, *Nat. Phys.* **2008**, *4*, 198–204.
- [4] M. Baumgarten, *Phys. Status Solidi B.* **2019**, *1800642*, DOI: 10.1002/pssb.201800642.
- [5] P. Ravat, Y. Ito, E. Gorelik, V. Enkelmann, M. Baumgarten, *Org. Lett.* **2013**, *15*, 4280–4283.
- [6] Y. B. Borozdina, E. Mostovich, V. Enkelmann, B. Wolf, P. T. Cong, U. Tutsch, M. Lang, M. Baumgarten, *J. Mater. Chem. C* **2014**, *2*, 6618–6629.
- [7] P. Ravat, Y. Borozdina, Y. Ito, V. Enkelmann, M. Baumgarten, *Cryst. Growth Des.* **2014**, *14*, 5840–5846.
- [8] Y. B. Borozdina, E. A. Mostovich, P. T. Cong, L. Postulka, B. Wolf, M. Lang, M. Baumgarten, *J. Mater. Chem. C* **2017**, *5*, 9053–9065.
- [9] P. V. Petunin, D. E. Votkina, M. E. Trusova, T. V. Rybalova, E. V. Amosov, M. N. Uvarov, P. S. Postnikov, M. S. Kazantsev, E. A. Mostovich, *New J. Chem.* **2019**, *43*, 15293–15301.
- [10] S. V. Klyatskaya, E. V. Tretyakov, S. F. Vasilevsky, *Russ. Chem. Bull.* **2002**, *51*, 128–134.
- [11] P. V. Petunin, E. A. Martynko, M. E. Trusova, M. S. Kazantsev, T. V. Rybalova, R. R. Valiev, M. N. Uvarov, E. A. Mostovich, P. S. Postnikov, *Eur. J. Org. Chem.* **2018**, *2018*, 4802–4811.
- [12] N. M. Gallagher, J. J. Bauer, M. Pink, S. Rajca, A. Rajca, *J. Am. Chem. Soc.* **2016**, *138*, 9377–9380.
- [13] P. R. Serwinski, B. Esat, P. M. Lahti, Y. Liao, R. Walton, J. Lan, *J. Org. Chem.* **2004**, *69*, 5247–5260.
- [14] E. A. Mostovich, Y. Borozdina, V. Enkelmann, K. Remović-Langer, B. Wolf, M. Lang, M. Baumgarten, *Cryst. Growth Des.*, **2012**, *12*, 54–59.
- [15] P. Ravat, Y. Teki, Y. Ito, E. Gorelik, M. Baumgarten, *Chem. Eur. J.*, **2014**, *20*, 12041–12045.
- [16] H. Tsujimoto, S. Suzuki, M. Kozaki, D. Shiomi, K. Sato, T. Takui, K. Okada, *Chem. Asian J.* **2019**, *14*, 1801–1806.
- [17] L. Noodleman, *J. Chem. Phys.* **1981**, *74*, 5737–5743.
- [18] L. Noodleman, E. R. Davidson, *Chem. Phys.* **1986**, *109*, 131–143.
- [19] K. Yamaguchi, F. Jensen, A. Dorigo, K. N. Houk, *Chem. Phys. Lett.* **1988**, *149*, 537–542.
- [20] T. Soda, Y. Kitagawa, T. Onishi, Y. Takano, Y. Shigeta, H. Nagao, Y. Yoshioka, K. Yamaguchi, *Chem. Phys. Lett.* **2000**, *319*, 223–230.
- [21] Crystallographic data for the structure of Form I and II of compound **1** have been deposited to the Cambridge Crystallographic Data Centre as supplementary publication no. CCDC 1938993-1938994. Copy of the data can be obtained, free of charge, on application to CCDC, 12 Union Road, Cambridge CB21EZ, UK (Fax: +44 122 3336033 or e-mail: deposit@ccdc.cam.ac.uk; Homepage: <https://www.ccdc.cam.ac.uk>).

Manuscript received: December 6, 2019
Revised manuscript received: December 12, 2019
Accepted manuscript online: December 14, 2019